Bulg. J. Phys. **40** (2013) 348–360

Surface Effects in Superparamagnetic Magnetite Particles*

I. Nedkov[1], **L. Slavov**[1], **B. Blagoev**[1], **K. Krezhov**[2]

[1]Institute of Electronics, Bulg. Acad. Sci., 72, Tsarigradsko Chaussee, 1784 Sofia, Bulgaria

[2]Institute for Nuclear Research and Nuclear Energy, Bulg. Acad. Sci., 72, Tsarigradsko Chaussee, 1784 Sofia, Bulgaria

Abstract. We have studied the properties of unshielded and shielded (hybrid) nanosized spherical magnetite particles with diameter 10 ± 2 nm, which are superparamagnetic at room temperature, through magnetometry, X-ray powder diffraction, magnetic force microscopy imaging and Mössbauer spectroscopy. The unshielded material was prepared by co-precipitation either in air or in inert atmosphere and part of it was shielded subsequently by β-cyclodextrin (β-$C_{42}H_{70}O_{35}$). The studies indicated that in the unshielded particles there is a surface layer with a depth of 3 nm wherein an exponential rise in the number of vacancies is observed in the octahedral sublattice ([B]-sites), so that the particle surface is highly defective and could be represented by the general formula $(Fe^{3+})_A[Fe^{3+}_{5x}Fe^{2.5+}_{2-6x}\Box_x]_BO_4$, where $x = 0$–0.3 and $\Box$ denotes vacancies. In contrast, the hybrid particles, being protected from oxidation, are structurally close to bulk magnetite so that the surface magnetic effects could be understood as due to the chaotic orientation of the magnetic moments at the magnetic–non-magnetic material interface. An empirical model for a spherical single domain particle was developed in attempting to describe the evolution of structural defects in the surface layer.

PACS codes: 75.75.-c; 71.30+h

1 Introduction

The development of nanotechnologies in the last decade has posed once again an old question related to the so-called metal-insulator transition at around 120 K that was discovered for magnetite by Verwey [1]. At room temperature, magnetite is an inverse spinel with simple cubic unit cells with two sublattices for iron cations in a nearest-neighbor arrangement: A – tetrahedral and B – octahedral. The general formula is written as $(Fe^{3+})_A[Fe^{2+}, Fe^{3+}]_BO_4$. The crystallographic unit cell is composed of 8 such formulae with 24 iron cations and

*Talk given at the Second Bulgarian National Congress in Physics, Sofia, September 2013.

 1310–0157

32 oxygen anions. Below the transition mentioned, in the bulk magnetite there appears a monoclinic unit cell which contains 32 formula units in comparison with the ones required for the inverse spinel. The distortion is very small and can be easily calculated. A number of interpretations has been offered concerning the nature of this transition. Basically, they belong to two groups, namely, those assuming the electrons transition as a primary deviation, and those proposing that the spatial transition is primary and causes the electrons transition as a consequence [2]. The changes in the spatial ordering of the magnetic cations inevitably affects the magneto-crystalline anisotropy of magnetite, so that the nanosized spherical particles can be considered as being a model structure in clarifying the magnetic interactions contribution on a nanosize scale to the possibility for appearance of a Verwey transition. The magnetic properties of a nanostructured superparamagnetic particle are strongly dependent on the surface layer. The interpretation of this influence vacillates between a critical "finite size effect" [3] and "surface spin disorder" [4]. In 1996, Kodama and Berkowitz [5] proposed a model of ferromagnetic spherical particle surrounded by a surface layer – a "canted" layer, which can be considered as being a second magnetic phase having the properties of spin glass; this leads to anisotropic exchange interactions between the two phases.

This work presents studies on the magnetic properties of unshielded and shielded (hybrid) nanosized spherical magnetite particles with diameter 10 ± 2 nm, which are superparamagnetic at room temperature. Superparamagnetism, or a collective paramagnetic effect, means that such particles possess a stable magnetic moment only in the presence of an applied magnetic field, or at low temperatures. We investigated the magnetic properties of nanoparticles where deviations are present or absent near the Verwey transition (about 120 K). The particles' superparamagnetic properties were also studied by Mössbauer spectroscopy. We focused our attention on characteristics related to magnetic phenomena – the magnetization curve of superparamagnetic particles, magnetic losses in a d.c. magnetic field and the appearance of a nonlinearity in the a.c. magnetic response. Data from Mössbauer spectroscopy measurements are also used for assessing the effect of applying soft-chemistry methods for preparing shielded and unshielded magnetite in an inert (nitrogen) atmosphere.

2 Experiment

The nanosized unshielded magnetite material was prepared by co-precipitation [6]. Part of the magnetic material was shielded by β-cyclodextrin and a series of ferrofluids were prepared [7]. We studied both the unshielded material and the shielded (hybrid) nanosized magnetite obtained from the precipitated fraction of the ferrofluids. A detailed characterization of these materials can be found in the articles cited [6,7]. This work was focused on the magnetic deviations related with the structural particularities of these particles. Beside various mag-

netic investigations, X-ray structural analysis, MFM imaging and Mössbauer measurements were conducted.

The magnetic properties were explored by a magnetic property measurement system (MPMS), a SQUID magnetometer and physical property measurement system (PPMS) (Quantum Design). The five-segment magnetic hysteresis up to 5.5 T at 80 K and 300 K was measured for both the shielded and unshielded magnetite particles. The magnetization *vs.* temperature curve in a d.c. magnetic field was also obtained. First, the samples were (quickly or slowly) cooled down to 4 K without a magnetic field being applied and when the temperature was stabilized, a single d.c. magnetization was measured. Afterwards, a d.c. magnetic field of 100 Oe was applied. Then, the magnetization was measured when increasing the temperature up to 300 K (ZFC curve) and again, when decreasing the temperature down to 4 K (FC curve). Finally, at 4 K the magnetic field was switched off (in a mode without overshoots) and the magnetization was measured again as the temperature was increased up to 300 K (remanence curve Rem). Additionally, the real and imaginary part of the a.c. magnetization (ACM) of shielded magnetite was obtained in the temperature interval from 4 to 300 K in a magnetic field with amplitude 10 Oe and frequency 1 kHz.

3 Results and Discussion

XRD data shows that magnetite is single-phase, while HRTEM demonstrates that the particles are spherical with a diameter of 10 ± 2 nm [6,7]. In our previous studies [6,9], we have found that the particles' surface is characterized by a defective layer extending to a depth of 3 nm, where one observes an exponential rise of the number of vacancies in the octahedral sublattice in a direction towards the surface. These defects are brought about by the oxidation processes. To minimize the critical oxidation effect, two approaches can be used: (i) minimizing the magnetite/atmospheric air contact by performing the synthesis process in an inert (nitrogen) atmosphere, or (ii) covering the magnetic nanoparticles by a layer of specific organics, which, besides hindering the oxidation, assists in separating the particles from agglomeration.

Figure 1 presents Mössbauer spectra of samples of nanosized magnetite prepared in nitrogen ambient.

One of the goals of the present experimental work was to complete a technological cycle while eliminating the product/air contact during the synthesis thus minimizing the structural changes on the magnetite particles' surface. On the other hand, the process results should not have been worse than those already achieved [6] in what concerns other important parameters of the end product, namely, dispersity and homogeneity. The unprocessed spectra shown in Figure 1 reveal precisely a worsened particles' size homogeneity as compared with that of particles prepared under normal conditions. The appearance of a magnetic

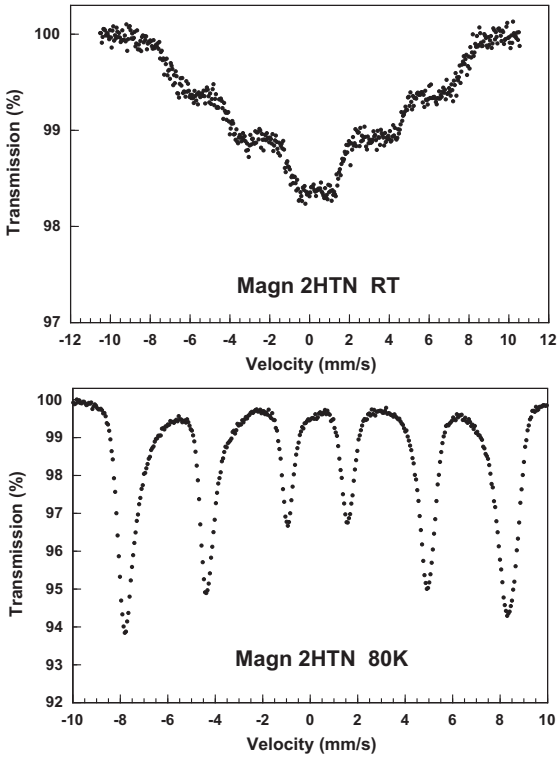

Figure 1. Mössbauer spectra (RT and 80 K) of magnetite particles prepared in nitrogen ambient.

sextet in the sample's RT spectrum is indicative of the presence of larger-size ferrimagnetic particles. The sample's spectrum at low temperature (80 K) is similar to that of maghemite (γ-Fe_2O_3), so that no distinction can be made between non-stoichiometric magnetite and maghemite. Such a combination leads to the signals from the tetra- and octahedral sublattices being overlapped, which complicates further the identification of the spectra obtained at such temperatures.

Figure 2 shows the RT Mössbauer spectrum of a sample of nanosized magnetite prepared in an inert atmosphere and shielded subsequently by an organic agent (β-cyclodextrin).

The spectrum consists of a superparamagnetic doublet with a quadrupole splitting of 0.50 mm/s and a relaxation section representing the beginning of a magnetic sextet. Compared with the unshielded sample, these hybrid particles exhibit a better homogeneity, while the lower value of the quadupole splitting indicates a magnetic phase that is better preserved. Nevertheless, in comparison

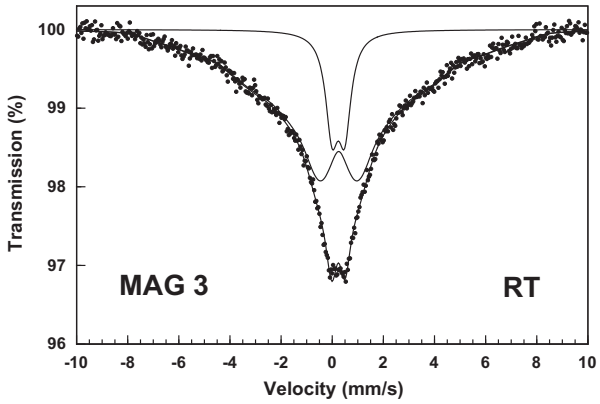

Figure 2. RT Mössbauer spectrum of a sample with organic shield.

with the RT spectrum of magnetite prepared under normal conditions [6], the presence of a relaxation part reveals a slightly larger particles' size. This could be due to negligible differences in the preparation conditions, which, in the case of such critically small sizes, might produce a significant effect.

The above studies of magnetite prepared in an inert atmosphere demonstrate the nanosized materials' strong sensitivity to the preparation conditions. The lack of atmospheric oxygen and its replacement by an inert (nitrogen) flow results in a worsening in the system's dispersity in both synthesis approaches. It thus appears that the growth of the iron oxide particles is affected by the oxygen diffusing from the atmospheric air through the liquid medium, the effect being a better and more homogeneous structuring of the particles. Analyzing the results, one can assume that the atmospheric oxygen's role is not merely negative, expressed in a disturbed stoichiometry on the particles' surface, but positive as well, namely, improved size homogeneity.

The data of the X-ray structural analysis of unshielded and shielded by β-cyclodextrin hybrid particles, produced under normal conditions, indicate that both types of powders are single phase. Table 1 compares X-ray data for bulk magnetite and the samples under investigation, showing that the lattice parameters of the particles produced are close to those of bulk magnetite.

Table 1. X-ray structural analysis data for single-crystal bulk magnetite and the particles studied

Type of material	Crystallographic system /PS	Lattice constant	Oxygen parameter
Single crystal bulk magnetite	Cubic	$a = 0.8389 \pm 0.001$	$u = 0.379 \ \pm 0.001$
Unshielded Fe_3O_4	Cubic	$a = 0.8352 \pm 0.0001$	$u = 0.3792 \pm 0.0001$
Shielded(hybrid) Fe_3O_4	Cubic	$a = 0.8379 \pm 0.0001$	$u = 0.3795 \pm 0.0001$

The particles' superparamagnetic nature at room temperature was established by means of Mössbauer spectroscopy. The measurements of unshielded magnetite taken at room temperature show the presence of 100% superparamagnetic particles with a doublet splitting (Figure 3). A doublet $\Delta E_Q \approx 0.6$ mm/s, which is indicative of the presence of a second, maghemite-like phase, has also been reported by other authors [10,11]. There have also been works [12] reporting the presence of a superparamagnetic singlet in the Mössbauer spectrum at 227 K of magnetite with particles size of 6 nm.

Using ILEEMS [6], we showed that the nanostructured magnetite particles with a diameter of 10 ± 2 nm prepared in air by a "soft-chemistry" technique have an oxidized surface of a defective spinel structure with vacancies in the octahedral sublattice and a general formula:

$$(\mathrm{Fe}^{3+})_{\mathrm{A}}[\mathrm{Fe}^{3+}_{5x}\mathrm{Fe}^{2.5+}_{2-6x}\square_x]_{\mathrm{B}}\mathrm{O}_4$$

where $\square$ is a vacancy structurally limited to $= 0$–0.2.

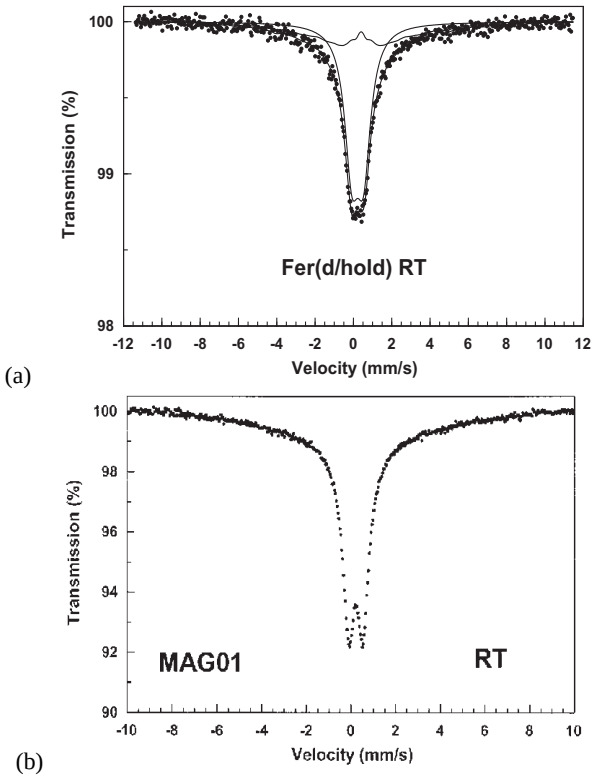

Figure 3. Mössbauer spectra at room temperature of: **()** hybrid particles with magnetic core size 10 ± 2 nm [9] and **(b)** nanostructured magnetite with grain size 10 ± 2 nm, [9].

This deviation was observed to a depth of 3 nm. This fact expands the concept of a "cant" surface layer and gives us grounds to consider the layer in question as a magnetic phase with magnetic exchange interactions different from those in the particle's core.

Figure 3.b presents a Mössbauer spectrum taken at room temperature of spherical magnetite particles encapsulated in β-cyclodextrin (β-$C_{42}H_{70}O_{35}$). The sample was a ferrofluid containing the hybrid particles dried on aluminum foil at room temperature and atmospheric pressure. The holder was filled during one week by about 1 ml of ferrofluid per day until the amount needed was reached. Although time-consuming, this preparation technique ensured both the possibility to study the sample at room temperature and to obtain a magnetic material in a state as close as possible to its state in the ferrofluid [9].

The spectrum at room temperature is typical for superparamagnetic particles with the doublet being very weakly expressed. Transition formations are also observed, which we relate to processes of partial agglomeration.

In contrast with the unshielded particles, the hybrid particles, being protected from oxidation, have no crystallographically defective surface layer, so that the surface magnetic effects are only due to the chaotic orientation of the magnetic moments at the magnetic−non-magnetic material interface.

Figure 4 presents hysteresis curves of shielded and unshielded magnetite at different temperatures. The magnetic moment of shielded magnetite is about 70% of the moment of the bulk single-crystal magnetite and is higher than that of unshielded magnetite (which is about 35% of the bulk magnetite's moment). Both types of magnetite particles were superparamagnetic without coercivity at room temperature. The hysteresis curve at 4 K shows pinched behavior near zero fields, which is a proof of the presence of a non-stoichiometric layer around non-encapsulated nanoparticles.

The curve of the d.c. magnetization *vs.* temperature is presented in Figure 5. For pure magnetite particles, there are only ZFC-FC curves measured by a SQUID magnetometer (black solid symbols), while for shielded magnetite we also include remanence (Rem) from SQUID (blank green symbols) and PPMS measurements (red (slow cooling) and blue (fast cooling) blank symbols).

For hybrid particles, the magnetization curves follow the typical behavior of superparamagnetic particles. The sample was first cooled down to 4 K without magnetic field and the magnetization was measured when the temperature was stabilized. Next, a d.c. magnetic field of 100 Oe was applied and the magnetization was measured at increasing temperature (ZFC). The initial value of the ZFC moments is relatively small, which means that the magnetic moments are frozen at this temperature (4 K). The magnetic moment increases as the temperature is raised and reaches a maximum at the blocking temperature (about 120 K, or the Verwey transition temperature). Next, the ZFC curve converges with the FC curve at the temperature of irreversibility. The magnetization is calculated

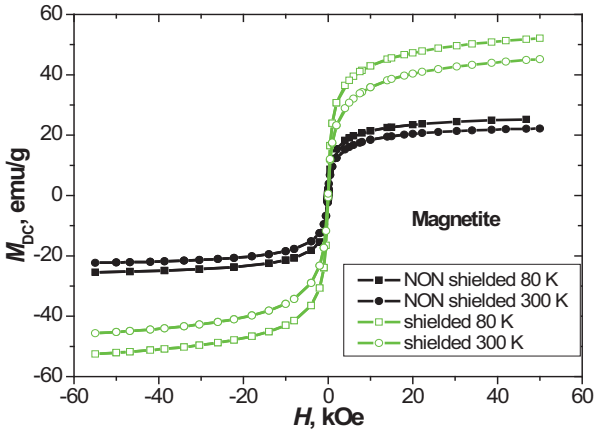

Figure 4. Magnetic hysteresis of β-cyclodextrin-shielded (blank green symbols) and unshielded (solid black symbols) magnetite.

in units of emu/g, where the signal for unshielded magnetite is divided by the magnetite powder's mass. The signal of the shielded magnetite is divided by the magnetite powder's mass plus the mass of the non-magnetic β-cyclodextrin. One can see the lower saturation magnetization values for unshielded particles. This confirms the existence of a crystal lattice perturbation on the surface of non-encapsulated magnetite particles. The fact that the shielded material originates from a stable ferrofluid, with the water content evaporating slowly in air, could lead to clustering and, thus, to particles of larger sizes.

The ZFC-FC-Rem magnetization for shielded magnetite was measured first on a SQUID in a fast cooling mode. It seen that the subsequent measurements of the d.c. magnetization of the same sample using the PPMS yielded a higher magnetic moment. Furthermore, we found a difference between the remanence curves' (d.c. magnetization without magnetic field at temperatures increasing from 4 to 300 K) behaviour measured by the SQUID and the PPMS systems. The SQUID remanence curve is typical for superparamagnetic particles [13,14]. Turning the magnetic field on causes a certain drop in the initial Rem magnetic moment followed by a slow decrease of the moment down to a negative value [13]. This low negative value of the magnetic moment could be due to the partially non-stoichiometric shield mentioned above. The absolute values of remanent magnetic moment at low temperatures as obtained by SQUID (blank green symbols) and PPMS (blank blue symbols) measurements in a fast cooling mode in both cases are the same but with opposite directions.

The difference in the d.c. magnetization curves (Figure 5) can be described as a history-dependent behavior. In the fast-cooling set of curves (blank blue symbols), the temperature transitions occur at a lower temperature and the magnetic

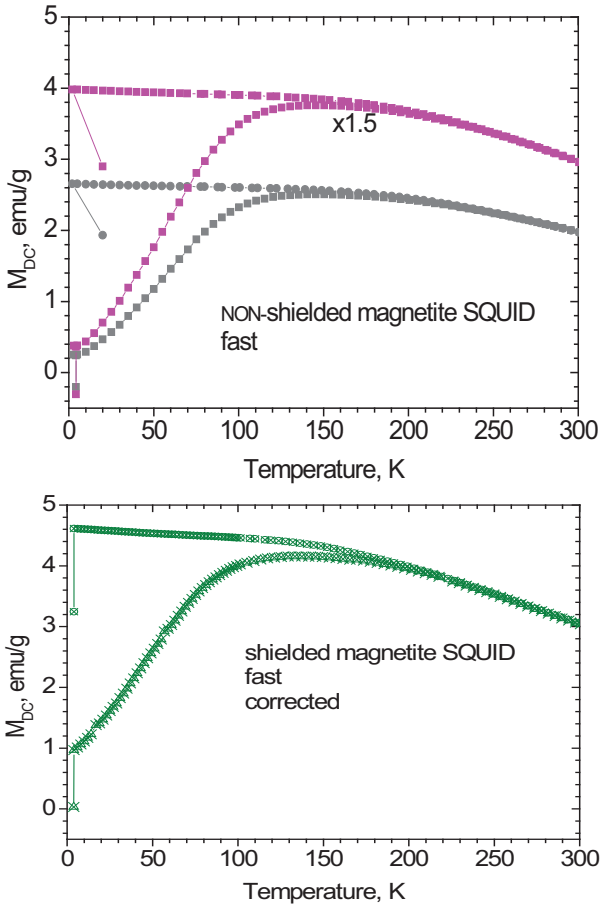

Figure 5. D.c. magnetization *vs.* temperature for unshielded and shielded nanostructured magnetite.

moment is somewhat higher than in the slow-cooling set curves (blank red and green symbols) (Figure 5). In the fast-cooling mode, the magnetic moments freeze so quickly that they cannot be rearranged and, therefore, the magnetic moment at low temperatures is higher. In the following slow heating, a strained lattice (fast-cooling mode) reaches its transition temperature before the relaxed lattice (slow-cooling mode).

It is known that the maximum of the ZFC curve for superparamagnetic particles is related with the blocking temperature. In our samples (shielded and unshielded magnetite), the maximum appears at a position where one could expect a Verwey transition to occur – T_V. According to the magneto-electronic model of the Verwey transition (Belov's theory), the valence electrons in mag-

netite are hoping electrons, while the inner ones are fixed on the A- and B-sublattice cations [15]. Below the Verwey transition (T_{V}), Vonsovskii exchange interactions between hoping electrons and cations arrange the hoping electrons antiferromagnetically to the B- sublattice cations (forming an electron sublattice), which results in a decrease of the net magnetization. As a first-order phase transition, the Verwey transition is characterized by a sharp cusp.

The difference between the initial ZFC and final FC magnetic moments values for the fast (blank blue symbols) and the slow (red open symbols) cooling modes (a factor of nearly two) could be due to a partially canted electron sublattice. In the slow cooling ZFC curve (blank red symbols), the electron sublattice is totally antiferromagnetic with respect to the B-cations sublattice, while in the fast cooling ZFC curve (blank blue symbols) some of the electrons in the electron sublattice are canted and, therefore, the net magnetization is higher. During the heating in a magnetic field (ZFC curves), the magnetic moments are being unfrozen and start a precession around the external magnetic field direction. This precession is stronger for canted electrons and, after the following slow cooling (FC curves), they freeze again in canted positions. The external magnetic field of 100 Oe is not sufficient (being much lower than the saturation magnetization – see Figure 4) to pin all magnetic moments to the field direction, but is sufficient to reduce nearly twice the canting effect.

The interparticles interactions are irreversible processes that are stronger and act at longer distances in the case of unshielded particles. When the particles are covered, the β-cyclodextrin shield reduces these interactions. In the low temperature region (below the maximum – T_b and T_{V}), where the magnetic moments are frozen in some preferred orientations, the particle to particle (p–p) and particle to field (p–f) interactions have finite values. A long-range ordering (LRO) takes place. When the temperature increases above T_b, the particles become superparamagnetic and the p–p and p–f interactions are reduced. The LRO changes to a short-range order (SRO). Upon heating, a temperature is reached at which the heating energy is comparable with the p–p and p–f interactions, namely, the irreversibility temperature T_{irr}. Therefore, the values of the T_b and the irreversibility temperature in unshielded magnetite are far from one another. For shielded magnetite, the irreversibility temperature is reached earlier because of the screening effect of the shield.

The real and imaginary part of the differential a.c. magnetization (ACMS) was measured using the PPMS after slow ZFC to 4 K (Figure 6) at magnetic field amplitude 10 Oe and frequency 1 kHz. The out-of-phase component (the ACMS imaginary part) showed maximum magnetic losses at 124.8 K, which is close to the Verwey transition temperature. For the in-phase component (the ACMS real part) the temperature of the maximum (214.6 K) is far from the value obtained by d.c measurements (138.2 K). In the case of d.c magnetization, the external magnetic field of 100 Oe is sufficient to reduce the maximum.

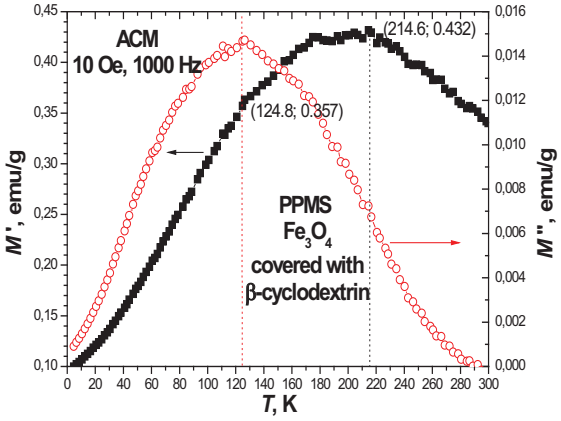

Figure 6. A.c. magnetization of shielded magnetite.

A non-linearity in the magnetic permeability near the Verwey transition was clearly observed for the hybrid particles only; we assume that such a transition cannot be seen in unshielded particles due to the disturbances in the magnetite particles' octahedral sublattice. More than 20% of the structure of an unshielded nanoparticle are characterized by a distrurbed octahedral sublattice and are in fact forming a different magnetic phase, which does not undergo the same changes at low temperatures as the particle's core. This effect is sensitive to the external magnetic field applied, so that, while an effective magnetic anisotropy exists in an unshielded particle, monoclinic deviations are present in an encapsulated magnetitite particle, which is the reason why one observes a well-expressed transition temperature. On the other hand, due to the particle's small volume, one may relate this non-linearity to the blocking temperature if () measurements are only performed. In the a.c. mesurements, this is a well-expressed effect that allows one to connect it with the Verwey temperature.

4 Conclusions

The nanoscale configuration and especially the monodomain state of magnetite at low temperatures are daunting in terms in the complexity of the current physical models and Verwey's simple charge-ordering model became more complicated due to the particles' surface modification. We observed changes in the magnetic properties of hybrid (magnetite/β-cyclodextrin) nanostructured superparamagnetic particles at 120 K, which we relate to the appearance of a Verwey transition. For comparison, we conducted measurements with unshielded particles of the same size prepared by the co-precipitation technique. The studies demonstrated that there exists in the latter type of particles a surface layer with a

depth of 3 nm where one observes an exponential rise in the number of vacancies in the octahedral sublattice, so that the particle surface is highly defective and can be represented by the general formula $(Fe^{3+})_A[Fe^{3+}_{5x}Fe^{2.5+}_{2-6x}\,\square_x]_BO_4$, where ?[U+2B1C] is a vacancy structurally limited to $= 0$–0.2. These deviations affect substantially the particle's magnetic properties – its magnetic moment is only 35% of that of bulk magnetite, although the XRD data point to a single-phase magnetite. We further observed a characteristic double peak in the Mössbauer spectrum at room temperature, which is a certain sign that no Verwey effect can be seen in such particles.

The so-called "cant" only exists in an encapsulated particle, which also leads to a decrease in the magnetic moment, but in this case it amounts to about 70% of that of the bulk material. The crystallographic deviations are insignificant and the superparamagnetic Mössbauer spectrum is not split.

In a non-encapsulated particle, the defective octahedral sublattice makes the transition difficult to detect. The incomplecte charge ordering of the octahedral iron cations, in combination with the ordering of the electron-orbital orientations of the ferrous cations and the lattice distortion, mask the effect. In contrast, when the particle is highly stoichiometric and possesses crystallographic parameters close to those of the single-crystal magnetite thanks to the protective organic shield, oxidation is avoided and a distinctive structural transition is seen at the Verwey temperature (about 120 K) even if the particle is superparamagnetic.

Acknowledgements

The work is supported by the Bulgarian National Fund under Contract DID 02/38/2009. Authors like to acknowledge the contribution of Prof. R.E. Vandenberghe and the Department of Subatomic and Radiation Physics at the University of Gent.

References

[1] E.J.W. Verwey (1939) *Nature* **144** 327.

[2] D.C. Mertens, W. Montfrooij, R.J. McQueeney, M. Yethiraj, J.M. Honig (2004) arXiv preprint cond-mat/0412375.

[3] S. Linderoth, P.V. Hendriksen, F. Bo, S. Wells, K. Davies, S.W. Charles, S. Mo (1994) *J. Appl. Phys.* **75** 6583-6585.

[4] F.T. Parker, F.E. Spada, T.J. Cox, A.E. Berkowitz (1995) *J. Appl. Phys*. **77** 5853.

[5] R.H. Kodama, A.E. Berkowitz, E.J. McNiff, S. Foner (1996) *Phys. Rev.Lett.* **77** 394.

[6] I. Nedkov, T. Merodiiska, L. Slavov, R.E. Vandenberghe, Y. Kusano, J. Takada (2006) *J. Magn. Magn. Mater.* **300** 358.

[7] L. Slavov, M.V. Abrashev, T. Merodiiska, Ch. Gelev, R.E. Vandenberghe, I. Markova-Deneva, I. Nedkov (2010) *J. Magn. Magn. Mater.* **322** 1904.

[8] Patent BG No. 65609, 2009.

[9] I. Nedkov (2007) *J. Optoelectron. Adv. Mater.* **9** 24.

[10] D.K. Kim, M. Mikhaylova, Y. Zhang, M. Muhammed (2003) *Chem. Mater.* **15** 1617.

[11] R.F.C. Marques, C. Garcia, P. Lecante, S.J.L. Ribeiro, L. Noé, N.J.O. Silva, V.S. Amaral, A. Millán, M. Verelst (2008) *J. Magn. Magn. Mater.* **320** 2311.

[12] S. Mørup, H. Topsøe, J. Lipka (1976) *J. de Physique, Colloque C6, Suppl. No 12* C6-287.

[13] Jim O'Brien (2004) Quantum Design Physical Property Measurement System PPMS users group, QD Magnetometers, presentation – Beijing.

[14] R. Prozorov, T. Prozorov, S.K. Mallapragada, B. Narasimhan, T.J. Williams, D.A. Bazylinski (2007) *Phys. Rev. B* **76** 054406.

[15] A.R. Muxworthy, E. McClelland (2000) *Geophys. J. Int.* **140** 101.